Heliyon 5 (2019) e02933

Contents lists available at ScienceDirect

Heliyon

journal homepage: www.cell.com/heliyon

Research article

Composition dependent structural phase transition and optical band gap tuning in InSe thin films

Harpreet Singh [a,b], Palwinder Singh [a,b], Randhir Singh [c], Jeewan Sharma [c], A.P. Singh [d], Akshay Kumar [c], Anup Thakur [b,*]

[a] Department of Physics, Punjabi University, Patiala, 147 002, Punjab, India
[b] Advanced Materials Research Lab, Department of Basic and Applied Sciences, Punjabi University, Patiala, 147 002, Punjab, India
[c] Department of Nanotechnology, Sri Guru Granth Sahib World University, Fatehgarh Sahib, Punjab, 140 407, India
[d] Department of Physics, Dr. B. R. Ambedkar National Institute of Technology, Jalandhar, Punjab, 144 011, India

ARTICLE INFO

Keywords:
Materials chemistry
Physical parameters
Chalcogenide
Optical band gap
Density of states
Phase transition

ABSTRACT

Bulk alloys of In_xSe_{100-x} (x = 5, 10, 20, 30, 40 and 50) are prepared using melt quenching technique. Thin films having thickness ~750 nm of these prepared bulk alloys are fabricated using thermal evaporation technique on glass substrate. The as-deposited In_xSe_{100-x} thin films with $x \leq 40$ are amorphous and $In_{50}Se_{50}$ thin film is crystalline in nature verified from X-ray diffraction (XRD). The change in morphology of deposited thin films with indium content also verifies structural phase transition and found that the phase transition started with $x = 40$ which is not detected in XRD pattern. The drastic change in transmission is found with 50% indium content. $In_{50}Se_{50}$ thin film has less than 30% transmission whereas other films are highly transparent. Optical band gap is calculated using Tauc's plot and decrease in optical band gap is observed with indium content. The variation of optical band gap from 1.88 eV to 1.12 eV is achieved with indium content of 5%–50%. The structural transition and change in optical band gap depict that InSe thin films are potential candidates in various technological applications.

1. Introduction

Chalcogenide alloys, consisting of chalcogen elements (S, Se and Te) or these elements as major constituents, are gathering attention from researchers and technological world because of their wide range of applications. Chalcogenide alloys are important materials for technologically important devices, such as optical data storage [1, 2], phase change random access memory [3, 4], near-infrared transmission window [5, 6], electrical switching [7, 8], optical fiber [9], solar cell [10], xerography [11] etc.

Indium selenide (InSe) is an important material and it belongs to a special semiconductor alloys group III-VI. The structural, optical [12, 13, 14], electronic [15, 16] and electrical [17, 18, 19] properties of InSe have been studied by various researchers. It is a layered semiconductor made of stacked layers of Se–In–In–Se atoms [20]. InSe is a potential material for solar cell [21, 22, 23, 24], diode [25], electrical switching [26], nonlinear optics [27], photodetector [28, 29, 30], photoinduced structural transformations [14], strain engineering [31] and microelectronics [18]. InSe thin films have been deposited using various physical and chemical methods [13, 14, 32, 33].

The property contrast accompanied by phase transition is an important aspect of chalcogenide materials for various applications. The flexible structure of chalcogenide is responsible for this phase transition. The phase transition in chalcogenide thin films is achieved by vacuum annealing [34], pressure [35] etc. Such phase transition can also be achieved by incorporation of suitable dopant with proper content in chalcogenide alloys [36].

In the present research work, effect of indium content in InSe thin films is investigated in reference to structural and optical properties. Bulk alloys and thin films of In_xSe_{100-x} (x = 5, 10, 20, 30, 40 and 50) have been prepared using melt quenching and thermal evaporation, respectively. The structural properties of as-prepared In_xSe_{100-x} thin films are investigated using X-ray diffraction. The morphology of as-prepared thin films is studied using field emission scanning electron microscope. The transmission spectrum is analyzed and the optical band gap is calculated. Some physical parameters have also been calculated and an effort has been made to correlate these parameters with structural properties.

* Corresponding author.
E-mail address: dranupthakur@gmail.com (A. Thakur).

https://doi.org/10.1016/j.heliyon.2019.e02933
Received 5 February 2019; Received in revised form 19 June 2019; Accepted 25 November 2019

Table 1. Values of $< m >$, n_α, n_β, f, V and L for In_xSe_{100-x} (x = 5, 10, 20, 30, 40 and 50) thin films.

x	$< m >$	n_α	n_β	f	V	L
5	2.05	1.03	1.1	0.292	5.95	3.9
10	2.10	1.05	1.2	0.250	5.90	3.8
20	2.20	1.10	1.4	0.167	5.80	3.6
30	2.30	1.15	1.6	0.083	5.70	3.4
40	2.40	1.20	1.8	0	5.60	3.2
50	2.50	1.25	2.0	-0.083	5.50	3.0

2. Experimental details

Bulk alloys of In_xSe_{100-x} (x = 5, 10, 20, 30, 40 and 50) are prepared using melt quenching method [37, 38]. Here, x denotes the atomic-weight percentage of elements. Highly pure (5N) elements are purchased from Sigma-Aldrich. For each stoichiometry, elements are weighed according to atomic weight percentage and poured into the quartz amouples. These amouples are sealed using torch equipped with oxygen and liquefied petroleum gas under the base pressure of $\sim 5 \times 10^{-6}$ mbar to remove the possibility of any reaction of alloy with oxygen at elevated temperature. The sealed amouples are heated in the increasing order of the melting point of constituent elements and after that rocking is performed to ensure the homogeneity of the mixture. Heated and rocked ampoules are quenched in ice-water after 24 h. The ingot is powdered using mortal pestle. Thin films of In_xSe_{100-x} (x = 5, 10, 20, 30, 40 and 50) prepared alloys are deposited on pre-cleaned glass substrate using thermal evaporation method [11, 37] using the Hind High Vacuum system (Model: BC-300) under a base pressure better than 5×10^{-6} mbar. Thickness of deposited thin films is monitored *in-situ* using a digital thickness monitor (Hind High Vacuum, DTM-101). The structural properties of deposited thin films are checked by X-ray diffraction (XRD) using X-ray diffractometer (X'Pert PRO PANalytical) with radiation of Cu $K_{\alpha 1}$ (λ = 1.5406 Å). For morphological study, field emission scanning electron microscope (FE-SEM) images are obtained using Hitachi-SU8010 and the composition of films is estimated using energy-dispersive spectroscopy (EDS) with the help of Bruker XFlash, 6130. The optical transmission of as-deposited thin films is measured by double beam UV-visible-NIR spectrophotometer (Varian Cary-5000) in the wavelength range of 500–1200 nm.

3. Results and discussion

3.1. Physical parameters

In chalcogenide alloys, the variation in mean coordination number ($< m >$) is due to the change in local structure. The value of $< m >$ can be calculated using Eq. (1) for In_xSe_{100-x} (x = 5, 10, 20, 30, 40 and 50) binary alloys.

$$< m > = \frac{aN_{In} + bN_{Se}}{a + b} \quad (1)$$

where a and b denote the values of atomic percentages of indium and selenium, respectively. Here N_{In} and N_{Se} are the coordination number of indium and selenium, respectively. The values of average coordination number of In_xSe_{100-x} alloys are listed in Table 1. It is found that the value of $< m >$ increases with indium content in In_xSe_{100-x} binary alloy. In covalent solids, there are two main neighbor bonding configurations; one is the bond stretching and other is the bond bending. These bonding configurations can be related to the value of $< m >$. n_α, number of bond stretching constraint, is related with $< m >$ as $< m > /2$, and n_β, bond bending constraint, is related with $< m >$ as $2 < m > -3$. It is found that the values for n_α and n_β increases with indium content and are listed in Table 1.

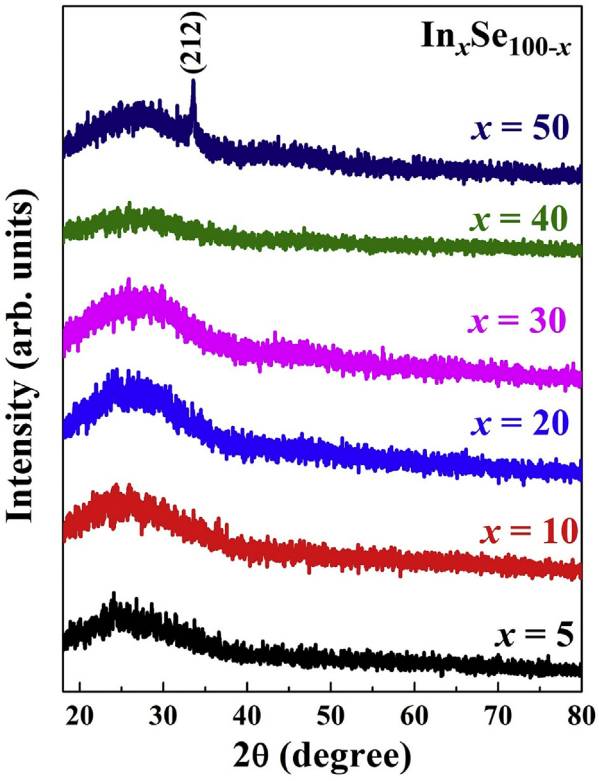

Figure 1. X-ray diffraction patterns of In_xSe_{100-x} (x = 5, 10, 20, 30, 40 and 50) thin films.

Chalcogenide alloys exhibit floppy or rigid region depending upon the value of $< m >$. The amount of floppy modes can be calculated using Eq. (2).

$$f = 2 - \frac{5}{6} < m > \quad (2)$$

The calculated values for the amount of floppy modes are tabulated in Table 1. It is observed that the value of f decreases with indium content.

Chalcogenide alloys exhibit structural relaxation due to the presence of lone pair of electrons. The number of lone pair of electrons is co-related with the vitreous state of chalcogenide alloys by Zhenhua [39]. Number of lone pair of electrons can be calculated using relation $L = V - < m >$, here L and V are the number of lone pairs of electron and valence electrons, respectively. The calculated number of lone pair of electrons is tabulated in Table 1. It is found that the number of lone pair of electrons decreased as indium content is increased in In_xSe_{100-x} alloy.

The increase in the values of $< m >$, n_α, n_β and decrease in f and L is also found with the incorporation of small amount of antimony in selenium [40]. The changes in physical parameters have also been observed in other chalcogenides with doping [41, 42].

3.2. Structural and morphological study

XRD patterns of as-prepared In_xSe_{100-x} (x = 5, 10, 20, 30, 40 and 50) thin films are shown in figure 1. It is clear from this figure that there is no sharp peak in XRD patterns of films with $x \leq 40$. This suggests that as-prepared In_xSe_{100-x} films with $x \leq 40$ are amorphous in nature. On the other hand, XRD pattern of $In_{50}Se_{50}$ film has a sharp peak at 33.6° which matches with the monoclinic phase [43, 44[45]] of InSe with space group P21. So, structural transition from the amorphous phase to crystalline

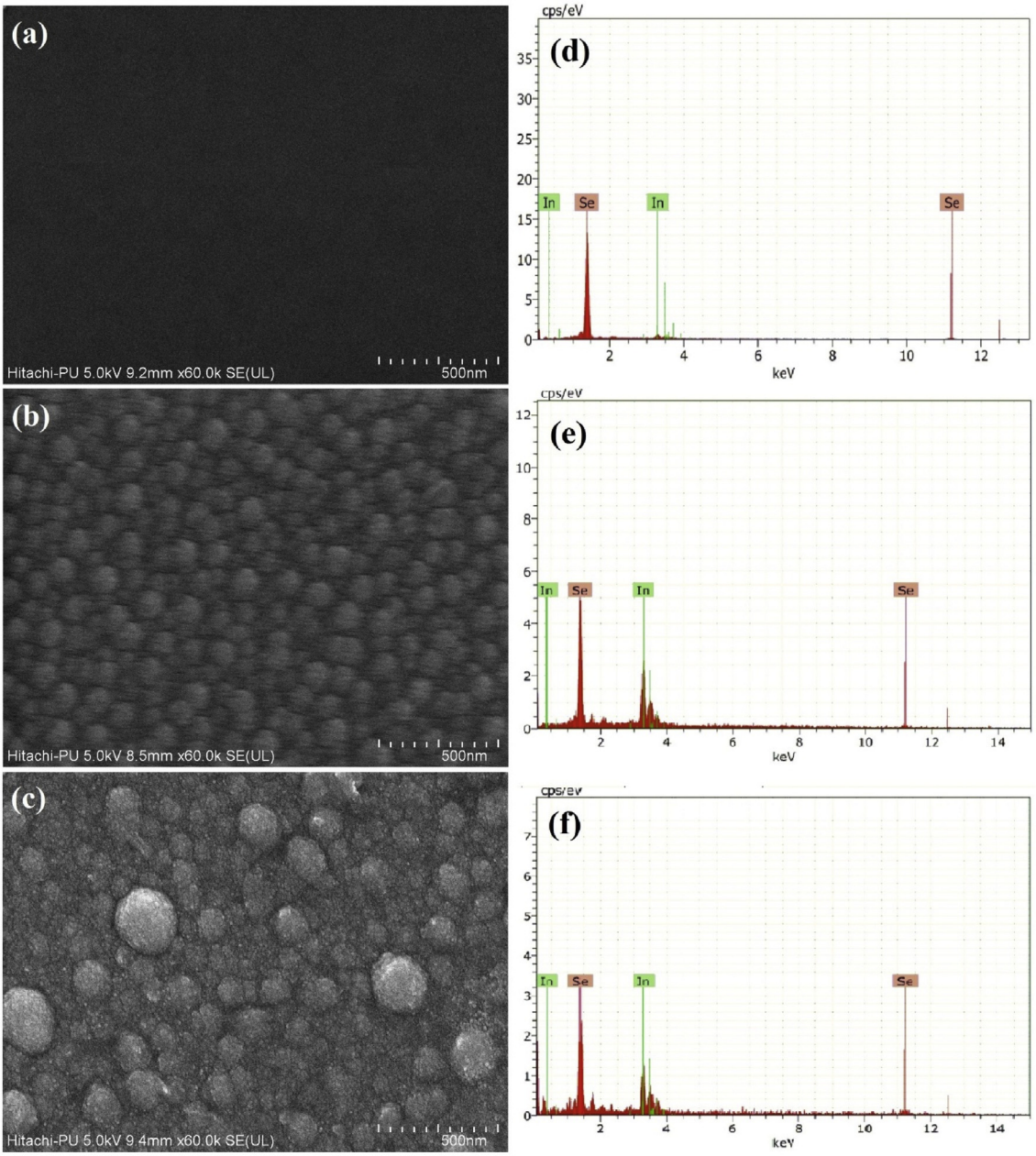

Figure 2. (a–c) Field emission scanning electron microscope images of In_xSe_{100-x} (x = 5, 40 and 50) thin films, respectively. (d–f) Energy dispersive spectra of In_xSe_{100-x} (x = 5, 40 and 50) thin films, respectively.

phase is achieved with higher indium content in In_xSe_{100-x}. The change in structure from amorphous to the crystalline phase of In_xSe_{100-x} thin films with indium content can be understood from change in the physical parameters (Table 1).

Figure 2 (a-c) show the morphology of as-deposited In_xSe_{100-x} ($x = 5$, 40 and 50) thin films. In_5Se_{95} thin film has uniform and smooth morphology without any growth of crystallites.

This also confirms the amorphous nature of thin film. The change in morphology is observed with higher indium content ($x = 40$). FE-SEM micrographs show that phase transition starts at $x = 40$, which is not detected through XRD. $In_{50}Se_{50}$ thin film has large crystallites compared to $In_{40}Se_{60}$. The drastic change in morphology confirms the phase transition from amorphous to crystalline phase in InSe thin films. Figure 2(d-f) show EDS spectra of as-deposited In_xSe_{100-x} ($x = 5$, 40 and 50) thin films, presence of indium and selenium X-ray peaks confirm the local composition of films.

3.3. Optical study

The optical transmission of as-deposited In_xSe_{100-x} ($x = 5$, 10, 20, 30, 40 and 50) thin films in the wavelength range of 500–1200 nm is shown in figure 3. The appearance of interference fringes are the signature of smooth and uniform films [46,47]. Thin films with indium content $x \leq 40$ are highly transparent with transmission more than 50%. But the drastic change in transmission is observed in $In_{50}Se_{50}$ film. $In_{50}Se_{50}$ film has transmission less than 30%. The decrease in transmission also confirms the phase transition in $In_{50}Se_{50}$ film. The decrease in transmission may be due to increase in scattering with In addition [48].

The optical transmission of In_xSe_{100-x} ($x = 5$, 10, 20, 30, 40 and 50) thin films shows a strong absorption edge in the wavelength region of 550–650 nm, but for $In_{50}Se_{50}$ it is around 800 nm. The strong absorption in the material normally occurs because of the band transitions of carriers. It is observed from figure 3 that the absorption edges show red shift

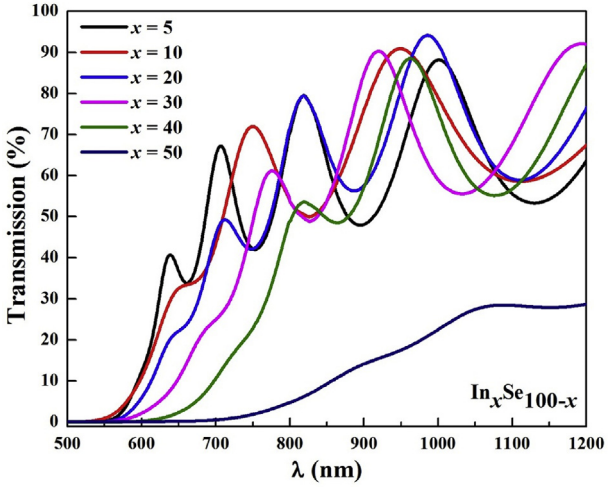

Figure 3. Transmission spectra of as-deposited In_xSe_{100-x} (x = 5, 10, 20, 30, 40 and 50) thin films.

with indium addition. The absorption coefficient (α) is inherent property of material which helps to derive other optical properties. It is calculated using the following relation [49]:

$$\alpha = \frac{1}{t}\ln\frac{1}{T} \tag{3}$$

where T is optical transmission and t is the thickness of film. The estimated thickness measured using DTM of as-prepared films is ~750 nm. The optical band gap can be calculated using the relation given by Eq. (4) known as Tauc's relation [50]:

$$\alpha h\nu = \beta\left(h\nu - E_g\right)^n \tag{4}$$

where $h\nu$, β and E_g denotes the photon energy, band tailing parameter and optical band gap, respectively. The parameter n can have different values depending upon the nature of transition. So, n can be 1/2, 2, 3/2 and 3 for direct allowed transition, indirect allowed transition, direct forbidden transition and indirect forbidden transition, respectively. From literature, the value of n is 2 used for InSe thin films [13,51,52]. Figure 4 shows the variation of $(\alpha h\nu)^{0.5}$ with energy for the thin films. The value of optical band gap is obtained from figure 4 and found that it changes significantly from 1.88 eV to 1.12 eV as indium content increases.

The values of optical band gap for In_xSe_{100-x} ($x = 5$, 10, 20, 30, 40 and 50) thin films can also be estimated theoretically [53] using Eq. (5):

$$E_g^{th}(PQ) = YE_g(P) + (1-Y)E_g(Q) \tag{5}$$

where Y denotes fraction of each element in the stoichiometry. For the stoichiometric alloy PQ, $E_g(P)$, $E_g(Q)$ and $E_g^{th}(PQ)$ are the values of optical band gap for elements P, Q and alloy PQ, respectively. The values for optical band gap for indium and selenium are used as 0.2 eV and 1.95 eV, respectively. The variation of optical band gap, calculated experimentally and theoretically, is shown in the inset of figure 4. It is clear from inset that experimentally and theoretically calculated values of optical band gap are in close agreement. The optical band gap of In_xSe_{100-x} thin films is comparable with another study [52]. The change in optical band gap with indium addition in amorphous thin films can be understood from density of localized states in the forbidden gap. The localized states in the forbidden band gap in chalcogenide alloys have been described through various models [54]. The presence of these localized states indicates the formation of defects, which originate due to valence band formation through lone pairs in chalcogenides. Thus, addition of indium in selenium matrix will give rise to additional absorption over a wide range of energy which leads to band tailing and shrinking of optical energy gap. The decrease in optical band gap in $In_{50}Se_{50}$ is because of change in phase from amorphous to crystalline [55].

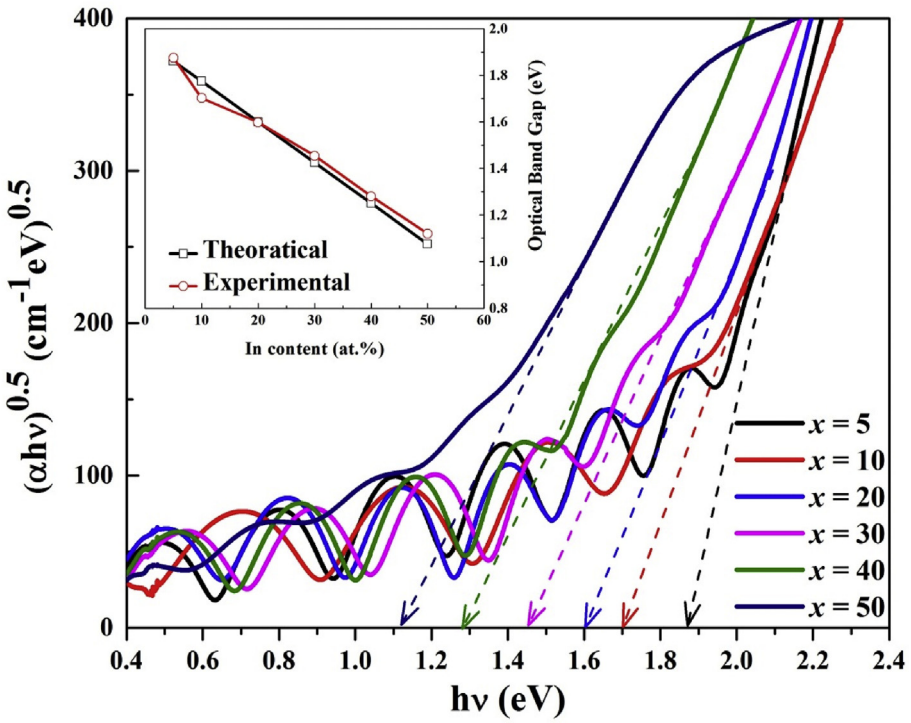

Figure 4. The variation of $(\alpha h\nu)^{0.5}$ with hν for In_xSe_{100-x} (x = 5, 10, 20, 30, 40 and 50) thin films. Inset shows the variation of experimentally observed and theoretically calculated optical band gap with indium content.

4. Conclusions

In_xSe_{100-x} (x = 5, 10, 20, 30, 40 and 50) bulk alloys and thin films (thickness ~750 nm) are prepared using melt quenching and thermal evaporation technique, respectively. X-ray diffraction patterns reveal that In_xSe_{100-x} with $x \leq 40$ thin films are amorphous in nature and phase transition from amorphous to crystalline has been achieved with $x = 50$ in $In_{50}Se_{50}$ thin film. The morphology of amorphous thin films is smooth and uniform. The drastic change in morphology is observed with structural transition. FE-SEM micrographs verify that the phase transition starts with $x = 40$. The drastic decrease in transmission at $x = 50$ also confirms the phase transition. The decrease in optical band was observed with indium content. The variation in optical band gap from 1.88 eV to 1.12 eV was observed. The structural transition and tuning in optical band gap present InSe thin films as a potential candidate in various technological applications.

Declarations

Author contribution statement

Anup Thakur, Harpreet Singh: Performed the experiments; Wrote the paper.

Palwinder Singh: Analyzed and interpreted the data; Wrote the paper.

Randhir Singh:Performed the experiments.

Jeewan Sharma, Abhinav Pratap Singh, Akshay Kumar: Analyzed and interpreted the data.

Funding statement

This work was supported by Department of Science and Technology, New Delhi under Research Project (Sanction No. SB/FTP/PS-075/2013 dated 29/05/2014). Palwinder Singh was supported by the Department of Science and Technology, New Delhi as SRF. Harpreet Singh was supported by the University Grant Commission, New Delhi as JRF, file no. 503864.

Competing interest statement

The authors declare no conflict of interest.

Additional information

No additional information is available for this paper.

References

[1] M. Wuttig, H. Bhaskaran, T. Taubner, Phase-change materials for non-volatile photonic applications, Nat. Photonics 11 (8) (2017) 465.
[2] S. Raoux, W. We lnic, D. Ielmini, Phase change materials and their application to nonvolatile memories, Chem. Rev. 110 (1) (2010) 240–267.
[3] L. Zhang, N. Miao, J. Zhou, J. Mi, Z. Sun, Insight into the role of W in amorphous GeTe for phase-change memory, J. Alloy. Comp. 738 (2018) 270–276.
[4] M. Pandian, P. Matheswaran, B. Gokul, R. Sathyamoorthy, K. Asokan, Preparation and characterization of indium chalcogenide thin films: a material for phase change memory, Appl. Surf. Sci. 449 (2018) 55–67.
[5] P. Singh, A.P. Singh, N. Kanda, M. Mishra, G. Gupta, A. Thakur, High transmittance contrast in amorphous to hexagonal phase of $Ge_2Sb_2Te_5$: reversible NIR window, Appl. Phys. Lett. 111 (26) (2017) 261102.
[6] P. Singh, A.P. Singh, J. Sharma, A. Kumar, M. Mishra, G. Gupta, A. Thakur, Reduction of rocksalt phase in Ag-doped $Ge_2Sb_2Te_5$: a potential material for reversible near-infrared window, Phys. Rev. Appl. 10 (5) (2018), 054070.
[7] M. Afifi, E. El-Metwally, N. Hegab, M. Mostfa, DC electrical conductivity and switching phenomena of amorphous $Te_{81}Ge_{15}Bi_4$ films, J. Alloy. Comp. 764 (2018) 498–504.
[8] N.A. Hegab, A.S. Farid, E. bd El-Wahabb, H. Magdy, Memory switching of chalcogenide glass $Se_{85}Te_{15}X_5$ (X= In, Sn) films, J. Alloy. Comp. 743 (2017) 36–43.
[9] L.A. Ketkova, M.F. Churbanov, Heterophase inclusions as a source of non-selective optical losses in high purity chalcogenide and tellurite glasses for fiber optics, J. Non-Cryst. Solids 480 (2018) 18–22.
[10] S.N.V.R. Manivannan, Preparation of chalcogenide thin films using electrodeposition method for solar cell applications-A review, Sol. Energy 173 (2018) 1144–1157.
[11] R. Kaur, P. Singh, K. Singh, A. Kumar, A. Thakur, Optical band gap tuning of Sb-Se thin films for xerographic based applications, Superlattice Microstruct. 98 (2016) 187–193.
[12] S.G. Choi, D.E. Aspnes, A.L. Fuchser, C. Martinez-Tomas, V.M. Sanjose, D.H. Levi, Ellipsometric study of single-crystal γ-InSe from 1.5 to 9.2 eV, Appl. Phys. Lett. 96 (18) (2010) 181902.
[13] M.M. El-Nahass, A.-B.A. Saleh, A.A.A. Darwish, M.H. Bahlol, Optical properties of nanostructured InSe thin films, Opt. Commun. 285 (6) (2012) 1221–1224.
[14] A.A.A. Darwish, Photoinduced effect in nanostructured InSe thin films for photonic applications, Opt. Commun. 310 (2014) 104–108.
[15] G.W. Mudd, M.R. Molas, X. Chen, V. Z_olyomi, K. Nogajewski, Z.R. Kudrynskyi, Z.D. Kovalyuk, G. Yusa, O. Makarovsky, L. Eaves, et al., The direct-to-indirect band gap crossover in two-dimensional van der Waals indium selenide crystals, Sci. Rep. 6 (2016) 39619.
[16] A. Politano, D. Campi, M. Cattelan, I.B. Amara, S. Jaziri, A. Mazzotti, A. Barinov, B. Gurbulak, S. Duman, S. Agnoli, et al., Indium selenide: an insight into electronic band structure and surface excitations, Sci. Rep. 7 (1) (2017) 3445.
[17] A.A.A. Darwish, M.M. El-Nahass, M.H. Bahlol, Structural and electrical studies on nanostructured InSe thin films, Appl. Surf. Sci. 276 (2013) 210–216.
[18] C.-H. Ho, Thickness-dependent carrier transport and optically enhanced transconductance gain in III-VI multilayer InSe, 2D Mater. 3 (2) (2016), 025019.
[19] D.A. Bandurin, A.V. Tyurnina, L.Y. Geliang, A. Mishchenko, V. Z_olyomi, S.V. Morozov, R.K. Kumar, R.V. Gorbachev, Z.R. Kudrynskyi, S. Pezzini, et al., High electron mobility, quantum hall effect and anomalous optical response in atomically thin InSe, Nat. Nanotechnol. 12 (3) (2017) 223.
[20] J.F. S_anchez-Royo, G. Munoz-Matutano, M. Brotons-Gisbert, J.P. Martinez-Pastor, A. Segura, A. Cantarero, R. Mata, J. Canet-Ferrer, G. Tobias, E. Canadell, et al., Electronic structure, optical properties, and lattice dynamics in atomically thin indium selenide flakes, Nano Res. 7 (10) (2014) 1556–1568.
[21] G. Amato, C. Manfredotti, M. Meliga, W. Mellano, InSe photoelectrochemical solar cells, Sol. Cells 13 (1) (1984) 19–28.
[22] S.H. Kwon, B.T. Ahn, S.K. Kim, K.H. Yoon, J. Song, Growth of $CuIn_3Se_5$ layer on $CuInSe_2$ films and its effect on the photovoltaic properties of In_2Se_3/$CuInSe_2$ solar cells, Thin Solid 323 (1-2) (1998) 265–269.
[23] C.-H. Ho, Amorphous effect on the advancing of wide range absorption and structural-phase transition in γ-In_2Se_3 polycrystalline layers, Sci. Rep. 4 (2014) 4764.
[24] M. Teena, A.G. Kunjomana, K. Ramesh, R. Venkatesh, N. Naresh, Architecture of monophase InSe thin film structures for solar cell applications, Sol. Energy Mater. Sol. Cells 166 (2017) 190–196.
[25] A. Hirohata, J.S. Moodera, G.P. Berera, Structural and electrical properties of InSe polycrystalline films and diode fabrication, Thin Solid Films (1-2) (2006) 247–250.
[26] M.A. Kenawy, A.F. El-Shazly, M.A. Afifi, H.A. Zayed, H.A. El-Zahid, Electrical and switching properties of InSe amorphous thin films, Thin Solid Films 200 (2) (1991) 203–210.
[27] M. Yuksek, H.G. Yaglioglu, A. Elmali, E.M. Aydin, U. Kurum, A. Ates, Nonlinear and saturable absorption characteristics of Ho doped InSe crystals, Opt. Commun. 310 (2014) 100–103.
[28] T. Zhai, X. Fang, M. Liao, X. Xu, L. Li, B. Liu, Y. Koide, Y. Ma, J. Yao, Y. Bando, et al., Fabrication of high-quality In_2Se_3 nanowire arrays toward high-performance visible-light photodetectors, ACS Nano 4 (3) (2010) 1596–1602.
[29] C.-H. Ho, C.-H. Lin, Y.-P. Wang, Y.-C. Chen, S.-H. Chen, Y.-S. Huang, Surface oxide effect on optical sensing and photoelectric conversion of α-In_2Se_3 hexagonal microplates, ACS Appl. Mater. Interfaces 5 (6) (2013) 2269–2277.
[30] G.W. Mudd, S.A. Svatek, L. Hague, O. Makarovsky, Z.R. Kudrynskyi, C.J. Mellor, P.H. Beton, L. Eaves, K.S. Novoselov, Z.D. Kovalyuk, et al., High broadband photoresponsivity of mechanically formed InSe-graphene van der Waals heterostructures, Adv. Mater. 27 (25) (2015) 3760–3766.
[31] Y. Ma, Y. Dai, L. Yu, C. Niu, B. Huang, Engineering a topological phase transition in β-InSe via strain, New J. Phys. 15 (7) (2013), 073008.
[32] N. Benramdane, A. Bouzidi, H. Tabet-derraz, Z. Kebbab, M. Latreche, Optical constants of InSe and In_4Se_3 thin films in the far infrared region, Microelectron. Eng. 51 (2000) 645–657.
[33] H.M. Pathan, S.S. Kulkarni, R.S. Mane, C.D. Lokhande, Preparation and characterization of indium selenide thin films from a chemical route, Mater. Chem. Phys. 93 (1) (2005) 16–20.
[34] J. Sharma, R. Singh, H. Singh, T. Singh, P. Singh, A. Thakur, S.K. Tripathi, Synthesis of $SnSe_2$ thin films by thermally induced phase transition in SnSe, J. Alloy. Comp. 724 (2017) 62–66.
[35] A.V. Kolobov, J. Haines, A. Pradel, M. Ribes, P. Fons, J. Tominaga, Y. Katayama, T. Hammouda, T. Uruga, Pressure-induced site-selective disordering of $Ge_2Sb_2Te_5$: a new insight into phase-change optical recording, Phys. Rev. Lett. 97 (3) (2006), 035701.
[36] H. Singh, P. Singh, A. Thakur, T. Singh, J. Sharma, Nanocrystalline Zn_xTe_{100-x} (x = 0, 5, 20, 30, 40, 50) thin films: structural, optical and electrical properties, Mater. Sci. Semicond. Process. 75 (2018) 276–282.
[37] P. Singh, P. Sharma, V. Sharma, A. Thakur, Linear and non-linear optical properties of Ag-doped $Ge_2Sb_2Te_5$ thin films estimated by single transmission spectra, Semicond. Sci. Technol. 32 (4) (2017), 045015.
[38] P. Singh, A.P. Singh, A. Thakur, Thermal stability improvement and crystallization behavior of Ag doped $Ge_2Sb_2Te_5$ phase change materials, J. Mater. Sci. Mater. Electron. 30 (2019) 3604–3610.

[39] L. Zhenhua, Chemical bond approach to the chalcogenide glass forming tendency, J. Non-Cryst. Solids 127 (3) (1991) 298–305.
[40] P. Singh, R. Kaur, A. Kumar, A. Thakur, Structural and optical properties of Sb_xSe_{100-x} ($x = 0, 5$) thin films, Opt. Quant. Electron. 49 (9) (2017) 288.
[41] A.H. Ammar, A.M. Farid, S.S. Fouad, Optical and other physical characteristics of amorphous Ge-Se-Ag alloys, Phys. B Condens. Matter 307 (1-4) (2001) 64–71.
[42] A. Aparimita, M. Behera, C. Sripan, R. Ganesan, S. Jena, R. Naik, Effect of Bi addition on the optical properties of $Ge_{30}Se_{70-x}Bi_x$ thin films, J. Alloy. Comp. 739 (2018) 997–1004.
[43] J.-C. Tedenac, G.P. Vassilev, B. Daouchi, J. Rachidi, G. Brun, Low-temperature region of the In-Se system, Cryst. Res. Technol. 32 (4) (1997) 605–616.
[44] J.H.C. Hogg, The crystal structure of In_6Se_7, Acta Crystallogr. B27 (1971) 1630–1634.
[45] K. Cenzual, L.M. Gelato, M. Penzo, E. Parthe, Inorganic structure types with revised space groups. I, Acta Crystallogr. B 47 (4) (1991) 433–439.
[46] R. Naik, P.P. Sahoo, C. Sripan, R. Ganesan, Laser induced Bi diffusion in $As_{40}S_{60}$ thin films and the optical properties change probed by FTIR and XPS, Opt. Mater. 62 (2016) 211–218.
[47] M. Behera, S. Behera, R. Naik, Optical band gap tuning by laser induced Bi diffusion into As_2Se_3 film probed by spectroscopic techniques, RSC Adv. 7 (30) (2017) 18428–18437.
[48] R. Naik, R. Ganesan, K. Sangunni, Optical properties change with the addition and diffusion of Bi to As_2S_3 in the Bi/As_2S_3 bilayer thin film, J. Alloy. Comp. 554 (2013) 293–298.
[49] P. Singh, R. Kaur, P. Sharma, V. Sharma, M. Mishra, G. Gupta, A. Thakur, Optical band gap tuning of Ag doped $Ge_2Sb_2Te_5$ thin films, J. Mater. Sci. Mater. Electron. 28 (15) (2017) 11300–11305.
[50] J. Tauc, Optical properties and electronic structure of amorphous Ge and Si, Mater. Res. Bull. 3 (1) (1968) 37–46.
[51] M.M. El-Nahass, A.A.A. Darwish, E.F.M. El-Zaidia, A.E. Bekheet, Gamma irradiation effect on the structural and optical properties of nanostructured InSe thin films, J. Non-Cryst. Solids 382 (2013) 74–78.
[52] M. Ganaie, M. Zulfequar, Optical and electrical properties of $In_4Se_{96-x}S_x$ chalcogenide thin films, J. Alloy. Comp. 687 (2016) 643–651.
[53] S.S. Fouad, A theoretical investigation of the correlation between the arbitrarily defined optical gap energy and the chemical bond in $Te_{46-x}As_{32+x}Ge_{10}Si_{12}$ system, Vacuum 52 (4) (1999) 505–508.
[54] N.F. Mott, E.A. Davis, Electronic Processes in Noncrystalline Materials, Clarendon, Oxford, 1971.
[55] R. Panda, R. Naik, N.C. Mishra, Low-temperature growth of phase in thermally deposited In_2Se_3 thin films, Phase Transitions 91 (8) (2018) 862–871.